Genetically eliminating Purkinje neuron GABAergic neurotransmission increases their response gain to vestibular motion

Trace L. Stay[a], Jean Laurens[a], Roy V. Sillitoe[a,b,1], and Dora E. Angelaki[a,c,1]

[a]Department of Neuroscience, Baylor College of Medicine, Houston, TX 77030; [b]Department of Pathology and Immunology, Program in Developmental Biology, Baylor College of Medicine, Jan and Dan Duncan Neurological Research Institute of Texas Children's Hospital, Houston, TX 77030; and [c]Center for Neural Science, Tandon School of Engineering, New York University, New York, NY 10003

Contributed by Dora E. Angelaki, December 19, 2018 (sent for review November 2, 2018; reviewed by Freek E. Hoebeek and Abigail Person)

Purkinje neurons in the caudal cerebellar vermis combine semicircular canal and otolith signals to segregate linear and gravitational acceleration, evidence for how the cerebellum creates internal models of body motion. However, it is not known which cerebellar circuit connections are necessary to perform this computation. We first showed that this computation is evolutionarily conserved and represented across multiple lobules of the rodent vermis. Then we tested whether Purkinje neuron GABAergic output is required for accurately differentiating linear and gravitational movements through a conditional genetic silencing approach. By using extracellular recordings from lobules VI through X in awake mice, we show that silencing Purkinje neuron output significantly alters their baseline simple spike variability. Moreover, the cerebellum of genetically manipulated mice continues to distinguish linear from gravitational acceleration, suggesting that the underlying computations remain intact. However, response gain is significantly increased in the mutant mice over littermate controls. Altogether, these data argue that Purkinje neuron feedback regulates gain control within the cerebellar circuit.

cerebellum | vestibular | electrophysiology | internal model | transgenic mice

Determining one's position and movement in the world is a ubiquitous task for living organisms. For vertebrates, several senses are available to detect self-motion, notably vestibular and visual systems (1). The vestibular system faces a unique challenge in distinguishing different types of motion: changes in head orientation relative to gravity activate otolith hair cells in exactly the same way as linear translations. The parsimonious solution to this ambiguity is to combine information from the otoliths and semicircular canals to create dynamic internal estimates of the two distinct components of movement (2–7). In concept, a change in head tilt relative to gravity (or equivalently, the gravity vector on the head) is the cross product of the angular velocity sensed by the canals and the gravity vector. Integrating these changes over time and incorporating correction feedback to slowly align gravity toward the otolith net acceleration signal provides an accurate model of head tilt relative to gravity (7) ("tilt," Fig. 1*A*). This internal representation of gravitational acceleration can then be subtracted from the otolith net acceleration information to estimate translational acceleration ("translation," Fig. 1*B*).

The caudal cerebellar vermis, an important component of the vestibulo-cerebellum which receives direct afferents from the vestibular organs (8–13), is a likely candidate region for carrying out this multistage computation. Indeed, Purkinje neurons in these lobules (caudal IX and all of X, the uvula-nodulus) have been shown in macaques to respond selectively to linear translation or gravitational tilt changes (14–17). However, it has not been tested whether this selectivity requires feedback from the cerebellar cortex, as might be postulated based on the tight relationship between Purkinje neurons, target nuclei, and cerebellar inputs (18), particularly with dense Purkinje neuron collaterals specifically in lobules IX and X (19, 20). Furthermore, it is unclear whether these properties extend outside the vestibulo-cerebellum.

The mouse is an unsurpassed mammalian model system for performing precise genetic manipulations to target individual circuit elements that mediate evolutionarily conserved behaviors. We performed a conditional genetic mouse cross to generate $L7^{Cre}$;$Vgat^{flox/flox}$ mice, in which Purkinje neuron GABAergic output is specifically blocked (21). These mice retain morphologically intact cerebellar cell types, including the Purkinje neurons themselves, but show severe behavioral abnormalities on rotarod performance and footprinting assays. Anesthetized recordings show changes in the variability of firing of both Purkinje and cerebellar nuclear neurons, consistent with the blockage of normal Purkinje neuron output. We utilized this model line to probe whether Purkinje neuron output is necessary to perform the network computations that differentiate gravitational and inertial acceleration (Fig. 1*C*). Macaque monkeys and mice have homologous vestibular organs and cerebellar microcircuitry, but differ in the range of head movements (22). Thus, we first examined whether this computation is evolutionarily conserved and shared by the mouse cerebellum. Furthermore, we also tested whether these signals are carried by cells in vermal transverse zones other than the vestibulo-cerebellum. Determining the role of cerebellar cortical signaling in this fundamental self-motion computation tests one of the most prominent theories of cerebellar function: how it generates internal models for sensorimotor planning and timing.

Significance

One theory of cerebellar function proposes that it creates internal models for action planning, timing, and sensory processing. Purkinje neurons in the caudal vermis of macaques carry a model of gravitational and linear acceleration, and here we show that this computation is evolutionarily conserved and represented across multiple lobules of the rodent vermis. Further, we show that genetically blocking Purkinje neuron GABAergic output leaves this computational ability intact, but leads to increased response modulation amplitude. We conclude that Purkinje neuron feedback regulates gain control within the cerebellar circuit.

Author contributions: T.L.S., R.V.S., and D.E.A. designed research; T.L.S. performed research; J.L. contributed new reagents/analytic tools; T.L.S. and J.L. analyzed data; and T.L.S., R.V.S., and D.E.A. wrote the paper.

Reviewers: F.E.H., University Medical Center Utrecht; and A.P., University of Colorado School of Medicine.

Conflict of interest statement: The authors declare no conflict of interest.

[1]To whom correspondence may be addressed. Email: sillitoe@bcm.edu or da93@nyu.edu.

This article contains supporting information online at www.pnas.org/lookup/suppl/doi:10.1073/pnas.1818819116/-/DCSupplemental.

Published online February 5, 2019.

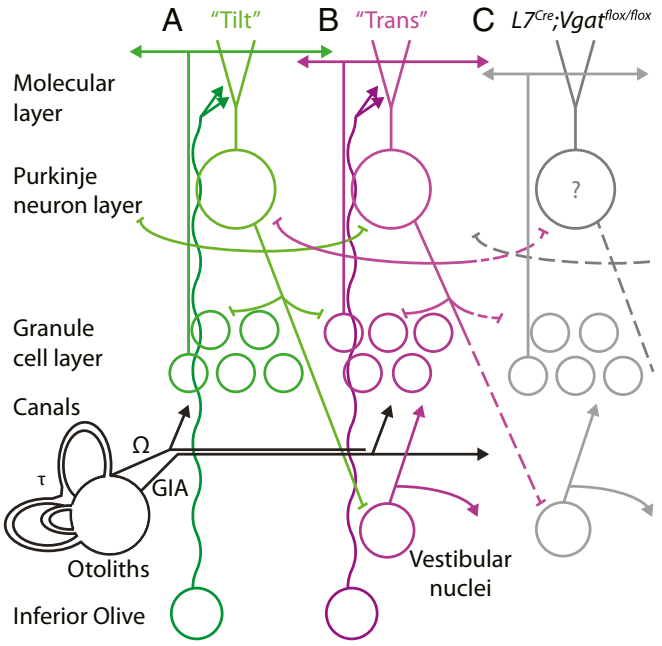

Fig. 1. Computation of self-motion components and genetic experimental design. (*A* and *B*) Schematic of simplified cerebellar circuit and conceptual theory of tilt-translation computation. (*A*) Head tilt relative to gravity (or gravitational acceleration vector, green) can be computed by integrating rotational velocity Ω from the semicircular canals, with canal signal decay time constant τ. Note that this integration can be implemented through a network of several cells and cell types rather than the individual cells depicted. (*B*) Translational acceleration ("Trans," magenta) can be calculated by removing the gravity signal from the net GIA acceleration communicated by the otoliths. (*C*) Genetically eliminating Purkinje neuron GABA signaling provides the ability to test whether Purkinje neuron signaling is necessary to distinguish tilt from translation within the cerebellar cortex. Some connections left off for visual simplicity, e.g., vestibular and inferior olive afferents in $L7^{Cre};Vgat^{flox/flox}$ mice.

Motion-Selective Purkinje Neurons Are Found Throughout the Posterior Half of the Mouse Cerebellum

We assessed cerebellar motion response selectivity in adult mice by recording during precisely controlled, multidirectional, acceleration-matched sinusoidal translation and tilt test stimuli (Fig. 2*A*). A total of 653 cells in 33 mice (22 male, 11 female) were given at least one test stimulus. Of these, we present quantitative analyses from 172 cells, which had apparent audible vestibular modulation, stable isolation through full testing along at least two stimulus directions (see below), and audible and/or visual evidence of complex spikes, signatures of putative Purkinje neurons (see *Materials and Methods* and *SI Appendix*). We focus on response properties of simple spikes, except for one analysis in section II below.

Motion stimuli (14–17) (see refs. 23 and 24 for more details) consisted of either linear (translation) motion alone, gravity-reorienting (tilt) motion alone, a cancellative condition ("tilt-translation"), where the net acceleration in the horizontal plane was zero, or an additive condition ("tilt+translation"), where the two types of motion summed together to double the net acceleration on the head (Fig. 2*B*). Using these four stimuli, in at least two orthogonal directions (typically more, when good isolation was maintained), allowed us to characterize each cell's vestibular properties, including preferred firing direction and phase, in the head's horizontal plane. In the present experiments, we also investigated whether Purkinje neurons in lobules VI-VIII could also be responsive to vestibular motion, despite being outside the area traditionally considered vestibulo-cerebellum (caudal lobule IX and lobule X).

We found neurons whose responses to vestibular motion were identical to what was previously reported in macaque uvula-nodulus (Fig. 2 *C–L*; see also refs. 16 and 17). Some cells responded to the net gravito-inertial acceleration (GIA, Fig. 2*D*). Similar to vestibular afferent mossy fibers, GIA-selective neurons modulated during both tilt and translation stimuli, with "matched" modulation amplitude, preferred direction and phase, such that their responses could be best modeled as the total sum of gravitational (tilt) and inertial (linear translation) components. Tilt-selective cells responded to tilt motion, irrespective of translation (Fig. 2*F*). We also identified translation-selective neurons, which responded solely to translation and not to tilt (Fig. 2*H*). Finally, other neurons modulated during both tilt and translation stimuli, but with "unmatched" modulation amplitude, preferred direction and phase (Composite neurons, Fig. 2*J*). These findings indicate that afferent vestibular information is transformed in mice in a manner similar to that reported in macaque monkeys (14–17).

Once signal quality showed signs of deteriorating in a mouse, the next motion-responsive cell recorded was electrolytically lesioned (*SI Appendix, Extended Materials and Methods*), allowing us to reconstruct the lobule(s) that neurons were recorded from (post hoc). Motion-selective neurons were found in all lobules VI-X (Fig. 2 *C–L* and *SI Appendix*, Table S1). For example, the highlighted GIA-responsive neuron was recorded from lobule VI (Fig. 2*C*), an example tilt cell from lobule VII (Fig. 2*E*), and an example translation cell from lobule IX (Fig. 2*G*). Motion-selective cells were found in both wild-type C57Bl/6J mice and littermates to the genetic mouse

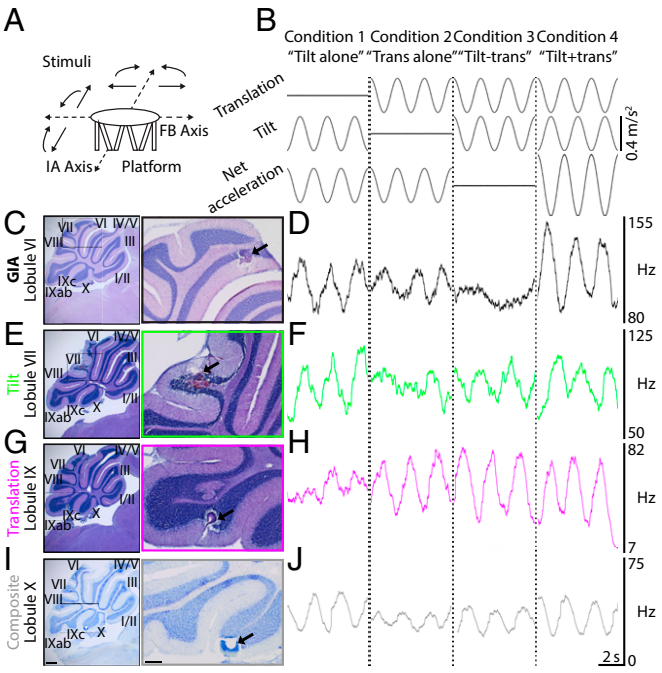

Fig. 2. Individual mouse Purkinje neurons in both central and caudal vermal lobules are selectively responsive to precise forms of self-motion. (*A*) Schematic of recording platform and linear acceleration or gravity-reorienting tilt stimuli. (*B*) Four stimuli of tilt alone, translation alone, tilt-translation, or tilt+translation motion were given along two or more directions. Net acceleration depicted on bottom row. (*C–J*) Recorded neurons marked by lesions in lobules VI, VII, IX, and X (arrows). (*C* and *D*) A gravito-inertial acceleration (GIA)-responsive neuron responded to tilt and translation but not to tilt-translation. (*E* and *F*) A tilt-selective neuron only responded during tilt. (*G* and *H*) A translation-selective neuron only responded during translation. (*I* and *J*) A composite neuron had intermediate responses to all four stimulus conditions; thus, it did not fit into one of the three motion-selective categories. (Scale bars in *C*, *E*, *G*, and *I*: *Left*, 500 μm, *Right*, 200 μm.)

cross; no differences were observed in firing properties between these mice (*SI Appendix*, Fig. S2 and subsequent sections below), so they are grouped together as "controls" henceforth.

To quantify neural response properties, we fitted each cell's firing rate with a "composite model" where the cell's response is modeled as a linear combination of tilt and translation, with different gain and phase along each axis of motion. We also examined the fit of each cell's response to three simple models: Tilt (including only tilt components), Translation (translation-only components), and GIA (where tilt and translation response components are matched; see *SI Appendix*, *Extended Materials and Methods* and refs. 16, 17, and 24). Cells were classified as tilt, translation, or GIA-selective if one of the three simple model categories provided a better fit than the other two simple models in more than 95% of bootstrapped resamples; otherwise, the cell was classified as composite (see *SI Appendix*, *Extended Materials and Methods* and ref. 24 for details).

The composite model provided a good fit to neuronal responses. Across the population of 128 neurons recorded in control mice, the median R^2 value was 0.57 (*SI Appendix*, Fig. S1). Since R^2 values are typically low in weakly or nonresponsive neurons, and our study aimed to examine the specific role of Purkinje neuron output on vestibular processing (rather than other functions), neurons with $R^2 < 0.25$ ($n = 15$) were excluded from quantitative analysis (as in ref. 17). Out of the 113 remaining neurons, 28 (25%) were "translation-selective," 31 (27%) were "tilt-selective," and 25 (22%) were "GIA-selective" (*SI Appendix*, Table S1). The remaining 30 cells (26%) were not significantly fit by any one of these three models and were classified as composite.

We used the composite model fits to compute response magnitude across the population. When tilt gain (expressed relative to gravitational acceleration G = 9.81 m/s^2) is plotted versus translation gain on a cell-by-cell basis, tilt- and translation-selective cells lie above and below the diagonal (Fig. 3*A*, green vs. magenta, respectively), whereas GIA and composite cells tend to lie close to the diagonal (Fig. 3*A*, black and gray). Tilt-selective cells were generally less responsive overall than translation-selective cells (Fig. 3*A* boxplots show mean gain [line], 95% confidence intervals [CI, boxes], and SDs [SD, whiskers]). Translation response gains averaged 127 (94–173 CI) spikes/s/G (translation cells), 20 (15–26 CI) spikes/s/G (tilt cells), 56 (42–76 CI) spikes/s/G (GIA cells), and 45 (35–59 CI) spikes/s/G (composite cells). Tilt response gains averaged 41 (31–54 CI) spikes/s/G (translation cells), 61 (51–73 CI) spikes/s/G (tilt cells), 58 (44–77 CI) spikes/s/G (GIA cells), and 57 (44–74 CI) spikes/s/G (composite cells). These values were remarkably similar to response gains measured in macaques (17): all cell types had approximately similar response gains during tilt, but widely different gains during translation. Note that although all recordings were made from the Purkinje neuron layer, only 31/128 (24%) could be definitively identified as Purkinje neurons based on their characteristic complex spike-triggered silencing of single spikes. Nevertheless, response properties were similar for putative and physiologically identified Purkinje neurons (*SI Appendix*, Fig. S2*B*).

Despite distinct modulation patterns, the population tilt/translation ratios did not differ from a unimodal distribution (Fig. 3*B*, Hartigan's dip test, $P = 0.96$). To test for clustering of cells into specific locations, we grouped cells according to their transverse zones (25, 26). Transverse zones differ in developmental origins, susceptibility to neurological defects, and gene expression patterns, making them a natural framework for examining potential functional differences. We analyzed cells in the central zone (lobules VI-VII), posterior zone (due to electrode penetration angles starting from lobule VI, the majority of these were the anterior transition area from caudal lobule VIII to rostral IX), and nodular zone (caudal lobule IX and lobule X). Similar-responding motion-selective neurons were found in all examined zones (Fig. 3 and *SI Appendix*, Table S1), without clear differences in distribution, though there appeared to be a trend toward more tilt cells in the central zone and more translation

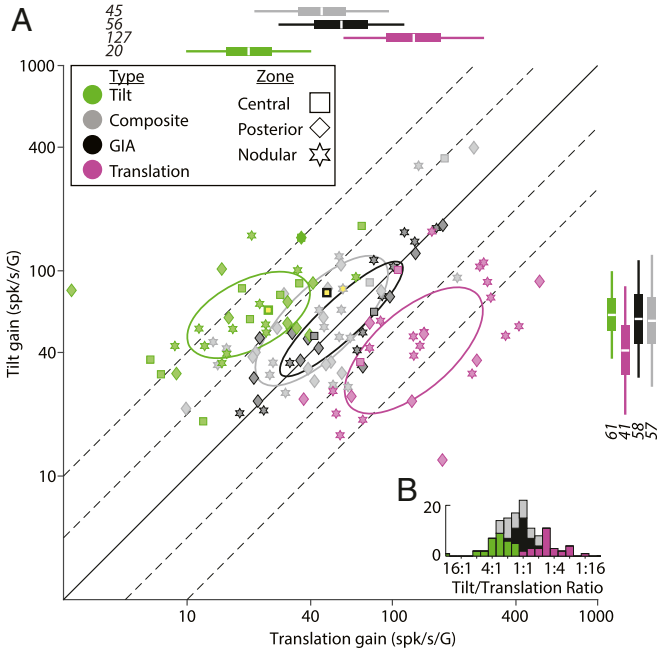

Fig. 3. The population of Purkinje neuron responses to tilt and translation motion does not differ from a unimodal distribution. (*A*) Each Purkinje neuron's ($n = 128$) response to translation plotted versus its response to tilt, with color and symbol indicating category and zonal classification. Green, gray, black, and magenta colors represent tilt-selective, composite, GIA-responsive, and translation-selective cells, respectively. Squares, diamonds, and stars represent central, posterior, and nodular zones, respectively. Yellow symbols indicate example cells from Fig. 2 *C*, *E*, and *I*. Ellipses indicate population means + one standard deviation. Boxplots indicate mean, 95% confidence intervals (boxes) and SDs (whiskers) for composite (gray), GIA (black), translation (magenta), and tilt (green) cells. (*B*) Histogram of tilt/translation gain ratios, with colors indicating neurons sorted into classes, as described above.

cells in the nodular zone (χ^2 test, $P = 0.036$). Neural responses were not significantly different in their fits to the linear models based on zone (mean R^2 values, central: 0.51 ± 0.4, posterior: 0.58 ± 0.03, nodular: 0.59 ± 0.02; one-way ANOVA, $P = 0.10$).

Cells classified as tilt-, translation-, or GIA-selective were encountered in all 21 control mice, suggesting that these results are robust to any potential effects of sample size. Due to the relatively large size of our electrolytic lesions and the mechanical limitations of the mediolateral spacing between electrodes, we were not able to reconstruct recording locations in the narrow, few-hundred-μm-wide parasagittal planes that organize the cerebellar cortex into zones. We conclude that Purkinje neurons throughout the posterior half of the cerebellar cortex encode tilt and translation self-motion, without an obvious relationship to transverse topography but with a potentially broader lobule distribution than previously appreciated (14–17).

L7^{Cre};Vgat$^{flox/flox}$ Purkinje Neurons Have Significantly Altered Spontaneous Firing Properties Compared with Control Purkinje Neurons, Including Higher Spiking Variability

Recognizing that Purkinje neurons represent the sole output of the cerebellar cortex, we focused on manipulating their output to test whether perturbing the vestibulo-cerebellar circuit as a whole would affect selective encoding of tilt and translation. We hypothesized this to have a major impact on vestibular processing, due to feedback projections from Purkinje neurons and vestibular nuclear cells (19, 20, 27). We utilized an *L7^{Cre};Vgat$^{flox/flox}$* conditional mouse line previously developed in our laboratory to spatially target the elimination of vesicular GABA transporter (*Vgat*) gene expression in Purkinje neurons (21). The cerebellum in this

mouse line can fire normal action potentials in Purkinje neurons, but because of the necessity of VGAT protein for loading GABA into synaptic vesicles (28–31), no GABA is released onto Purkinje neuron targets, leading to severe ataxia and disequilibrium.

We previously reported that $L7^{Cre};Vgat^{flox/flox}$ mice have significantly higher spiking variability in Purkinje neurons than littermate controls during anesthesia (21); therefore, we tested whether this difference in spontaneous physiology persists in awake mice. We examined median firing rates and median coefficients of variation 2 (CV2; see *SI Appendix*, *Extended Materials and Methods*) during rest periods absent of any stimuli in cells from 12 different $L7^{Cre};Vgat^{flox/flox}$ mice (Fig. 4*A*). One-way multivariate analysis of variance (MANOVA) analysis indicated a significant main effect of genotype on rate or CV2 together: $P = 0.0046$ (*SI Appendix*, Table S2). Consistent with what we found previously, variability in firing (CV2) was higher overall for $L7^{Cre};Vgat^{flox/flox}$ Purkinje neurons than controls (Fig. 4*B*; $L7^{Cre};Vgat^{flox/flox}$ median CV2 = 0.56 ± 0.02, control CV2 = 0.49 ± 0.01, Wilcoxon rank sum test, $P = 0.0024$), while no significant difference was detected in the overall firing rate ($L7^{Cre};Vgat^{flox/flox}$ firing rate = 56.6 ± 3.4 Hz, control firing rate = 62.5 ± 2.4 Hz, $P = 0.21$). This suggests that Purkinje neuron feedback is involved in regulating variability of firing in the cerebellar cortex in awake mice.

As noted, our analyses focused on Purkinje neuron simple spikes (SS), in line with previous studies on motion selectivity in the vestibulo-cerebellum (15–17). Although SS responses were the primary aim of the study, we also examined spontaneous complex spike properties for potential differences between control and $L7^{Cre};Vgat^{flox/flox}$ Purkinje neurons, as complex spikes are believed to be a key component of cerebellar learning and function. One-way MANOVA testing failed to show a significant difference between genotypes for median firing rate or CV2 ($P = 0.15$). Median complex spike firing rates in controls averaged 1.31 ± 0.16 Hz, versus 1.45 ± 0.25 Hz in $L7^{Cre};Vgat^{flox/flox}$ Purkinje neurons. Median complex spike CV2 values in controls averaged 0.90 ± 0.04 and in $L7^{Cre};Vgat^{flox/flox}$ Purkinje neurons 0.79 ± 0.02. Together, these data do not indicate any clear difference in spontaneous complex spike firing properties. We continued by examining other factors that could potentially influence SS firing.

Within each genotype, there were no significant differences in median simple spike firing rate between neurons recorded from different zones (Fig. 4*B*; central zone = 67.1 ± 8.4 Hz, posterior = 63.0 ± 3.6 Hz, nodular = 59.6 ± 2.9 Hz; $L7^{Cre};Vgat^{flox/flox}$ central = 56.1 ± 5.7 Hz, posterior = 52.1 ± 4.1 Hz, nodular = 51.6 ± 8.3 Hz), nor in CV2 (control central zone = 0.50 ± 0.03, posterior = 0.50 ± 0.02, nodular = 0.48 ± 0.02; $L7^{Cre};Vgat^{flox/flox}$ central = 0.46 ± 0.02, posterior = 0.44 ± 0.04, nodular = 0.53 ± 0.04; one-way MANOVAs, control mice: $P = 0.26$; $L7^{Cre};Vgat^{flox/flox}$ mice: $P = 0.30$). Additionally, we did not observe any difference in these spike statistics based on gender (female Hz = 63.7 ± 3.4, male Hz = 59.2 ± 2.4, Wilcoxon rank sum test, $P = 0.31$; female CV2 = 0.51 ± 0.02, male CV2 = 0.50 ± 0.01, $P = 0.80$) or age of the mice (age binned into "young," <120 d old, or "mature," >120 d old; young Hz = 60.2 ± 3.0, mature Hz = 61.2 ± 2.6, Wilcoxon rank sum test, $P = 0.84$; young CV2 = 0.50 ± 0.02, mature CV2 = 0.51 ± 0.02, $P = 0.86$). These properties were similar for putative and physiologically confirmed Purkinje neurons (*SI Appendix*, Fig. S2*A*). They did not differ in firing rate (confirmed Hz = 63.3 ± 3.5, putative Hz = 60.0 ± 2.4, Wilcoxon rank sum test, $P = 0.42$) or variability (confirmed CV2 = 0.47 ± 0.03, putative CV2 = 0.52 ± 0.01; $P = 0.04$). This similarity across Purkinje neurons allowed us to use population means to compare our conditional genetic mice with controls during vestibular stimuli (Fig. 5).

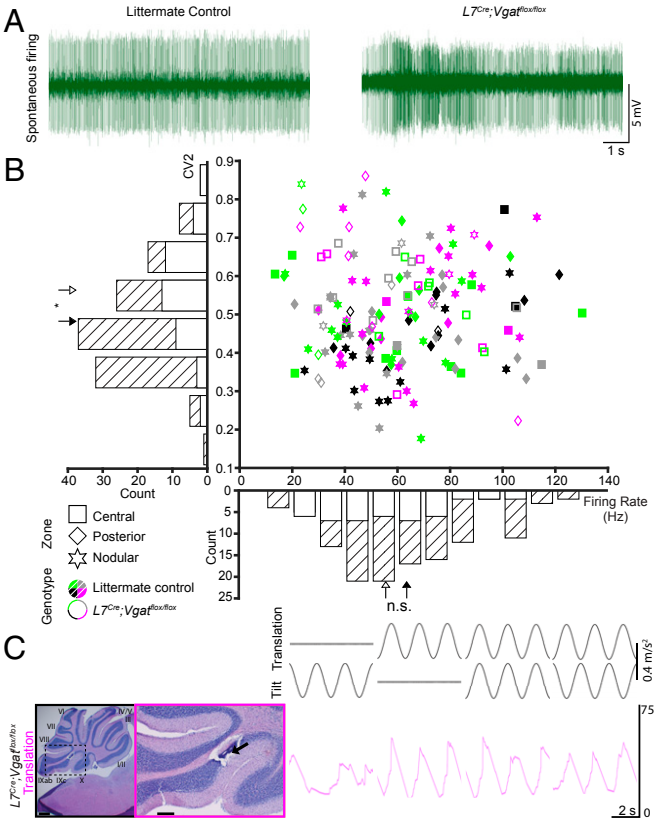

Fig. 4. $L7^{Cre};Vgat^{flox/flox}$ Purkinje neuron firing properties. (*A*) Examples of spontaneous raw firing traces from control and $L7^{Cre};Vgat^{flox/flox}$ Purkinje neurons demonstrating higher firing variability in the latter. (*B*) Spontaneous median firing rate for each control ($n = 128$) and $L7^{Cre};Vgat^{flox/flox}$ ($n = 43$) Purkinje neuron plotted vs. median CV2, with shape, color, and fill indicating zone, functional classification, and genotype. Shape and color scheme identical to Fig. 3. Filled symbols represent controls, while open symbols indicate $L7^{Cre};Vgat^{flox/flox}$ Purkinje neurons. Histogram summaries show CV2 and rate, with genotype means indicated by filled or open arrows, respectively. Significant difference in median CV2 between $L7^{Cre};Vgat^{flox/flox}$ neurons (hatched bars) and controls (open bars) indicated by asterisk ($P = 0.0012$), while no difference was seen in median firing rate ($P = 0.077$, Wilcoxon rank sum tests). No significant differences were observed between zones within either genotype. (*C*) Example of $L7^{Cre};Vgat^{flox/flox}$ Purkinje neuron response to applied vestibular stimuli. (Scale bar, L: 500 μm; R: 200 μm.)

Genetically Eliminating GABAergic Neurotransmission from Purkinje Neurons Increases Their Modulation Response to Self-Motion

Despite altered spontaneous firing properties, cerebellar neurons in $L7^{Cre};Vgat^{flox/flox}$ mice retained their selective response to tilt or translation motion (Fig. 4*C*). $L7^{Cre};Vgat^{flox/flox}$ Purkinje neurons classified as tilt-, translation-, or GIA-selective were found in all recorded lobules VI-IX (*SI Appendix*, Table S1). The small sample of neurons in each area limits the statistical power of any direct comparison of the zonal composition of each cell type between control and mutant mice, but there was a potential indication of a higher proportion of translation cells and fewer GIA cells in $L7^{Cre};Vgat^{flox/flox}$ mice (*SI Appendix*, Table S1). When the population responses to translation and tilt were plotted, the $L7^{Cre};Vgat^{flox/flox}$ mice showed a similar wide distribution of response selectivity as controls (Fig. 5 *A* and *B*). However, the response amplitude of these cells was much larger than in controls (Fig. 5*A* confidence intervals): the tilt response gain of tilt-selective cells increased from 61 spikes/s/G (spk/s/G) in controls to 216 spk/s/G in $L7^{Cre};Vgat^{flox/flox}$ mice (Wilcoxon rank sum test, $P = 5.2e\text{-}05$) whereas the translation response gain of translation cells increased from 127 spk/s/G to 287 spk/s/G ($P = 0.0015$). Likewise, both the tilt and translation gain of composite cells increased (tilt: from 57 to 115 spk/s/G; translation: 45–144 spk/s/G; $P = 1.9e\text{-}4$ and $2.3e\text{-}05$). Tilt gain and translation gain did not significantly differ between male and female mice (Wilcoxon rank sum test, tilt gain $P = 0.34$,

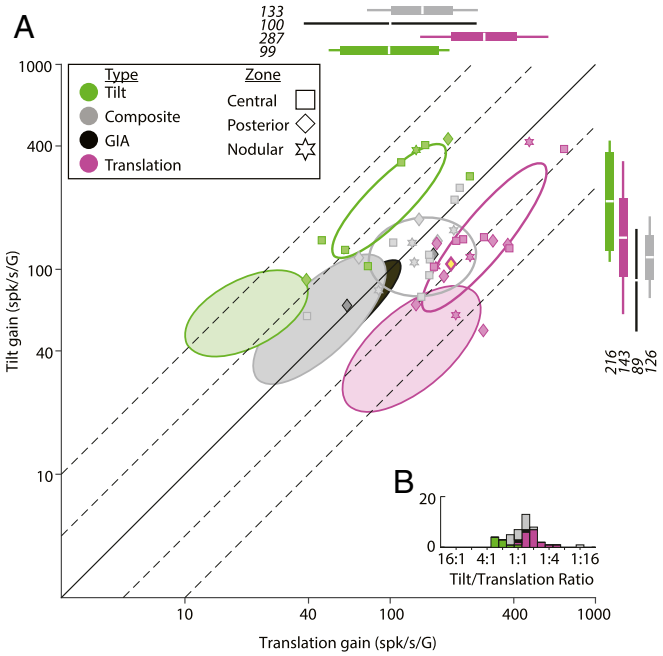

Fig. 5. Genetically eliminating Purkinje neuron *Vgat* expression increases their modulation response amplitude to self-motion. (*A*) Individual Purkinje neuron (n = 43) response to translation and tilt plotted as in Fig. 3, with color and symbol indicating classification type and transverse zone. Filled colored ellipses indicate group means for control cells as in Fig. 3, while unfilled ellipses and boxplots indicate group means for $L7^{Cre};Vgat^{flox/flox}$ Purkinje neurons. Yellow symbol indicates translation cell from anterior lobule IX shown in Fig. 4*C*. (*B*) Tilt/translation histogram for all $L7^{Cre};Vgat^{flox/flox}$ Purkinje neurons, as in Fig. 3.

trans gain $P = 0.22$). We conclude that inhibitory Purkinje neuron output, including its primary or secondary feedback onto the cerebellar cortex, is necessary for setting appropriate response levels for vestibular processing.

As secondary analyses, we also examined the preferred firing direction and phase of each cell in both $L7^{Cre};Vgat^{flox/flox}$ mice and controls (*SI Appendix*, Fig. S3). The preferred firing directions for preferred stimuli for tilt-, translation-, and GIA-responsive cells in controls were uniformly distributed (Rayleigh uniformity test, $P = 0.97$ [GIA], $P = 0.36$ [translation], $P = 0.97$ [tilt]). In $L7^{Cre};Vgat^{flox/flox}$ mice, translation- and GIA-responsive cells' preferred directions appeared uniformly distributed, while tilt cells' peak responses appeared to cluster along the forward-back axis (see legend of *SI Appendix*, Fig. S3), but a larger sample size of each functional group would provide the means to fully delineate functional compartmentalization. For response phase, Purkinje neurons in both $L7^{Cre};Vgat^{flox/flox}$ mice and controls clustered around specific components of movement, similar to what had been reported in macaque (17). Control tilt-, translation-, and GIA-selective cell peak responses tended to cluster around an average of $-10 \pm 11°$ relative to angular velocity, $0 \pm 15°$ relative to linear velocity, and $10 \pm 17°$ relative to linear acceleration, respectively ($P < 0.02$ for all types, Rayleigh uniformity test). $L7^{Cre};Vgat^{flox/flox}$ translation-selective cell peak responses clustered close to linear acceleration (average phase = $-61 \pm 15°$ relative to linear velocity, P = 7.3e-04), while tilt- and GIA-selective cell peak responses were not significantly clustered (P = 0.06, P = 0.22, respectively). While these analyses are constrained by the small sample size from each zone, they suggest that response phase to vestibular motion may also be affected in $L7^{Cre};Vgat^{flox/flox}$ Purkinje neurons.

Discussion

The existence of net tilt and translation-selective signals in cerebellar Purkinje neurons, originally identified in macaque monkeys (14–17), has been interpreted as evidence that the brain processes vestibular signals through an internal model of head movement. Here, we have shown that the mouse cerebellum performs similar computations. Although mice and macaques experience different head accelerations (22), their vestibular system shows similar properties (12, 13, 32, 33). Previous studies have identified motion responsiveness in lobules IX-X of mice (34–37), but none have employed controlled testing paradigms required to determine if cells were selectively responding to linear or gravity-reorienting motion. Our recordings have identified Purkinje neurons in mice, which display selective responses to tilt or translation (Fig. 3). Further, we found that the range of responsiveness of tilt- and translation-selective cells is largely similar to what was observed in macaques (17). These results suggest that the differentiation of tilt and translation is a fundamental computation across vertebrates that is likely resolved at early stages of vestibular processing.

Primary vestibular afferents have been reported to terminate in lobules IX-X in the mouse (12, 13). These studies have been supported with findings showing that lesions to the uvula-nodulus cause postural instability and imbalance (38), as well as erroneous gravity perceptions (39). Notably, we found motion-selective neurons in both lobules IX-X, as previously reported in macaques, as well as lobules VI-VIII (Fig. 2), which are not typically considered as vestibulo-cerebellum compartments. How these selective responses develop is not currently understood, but one possibility involves secondary vestibular projections ascending from the vestibular nuclei (27, 40, 41). Of note, the central and caudal transverse zones have tied developmental lineage (25, 42), suggesting that some aspects of their functions, e.g., appropriate circuit wiring, may be established early in embryogenesis. It would be interesting to examine whether motion responsiveness is also represented in the more anterior lobules, which were not sampled in this study.

The cerebellum is organized into a patterned array of modules that are defined by neuronal birth dates, developmental lineage, gene expression, afferent termination patterns and firing characteristics (43). We did not observe evidence for module-specific clusters of tilt- or translation-selective Purkinje neurons, and the tilt/translation sensitivity ratio did not differ from a unimodal distribution (Fig. 3). However, the module pattern in the caudal cerebellum is composed of very wide stripes that are interrupted by narrow ones (26). Our recordings were likely biased toward one class of Purkinje neurons. Future work would require more closely spaced electrodes to fully disentangle if there is a mediolateral organization of cell responses to tilt and translation.

We chose to silence Purkinje neurons chronically rather than with acute optogenetics, in part because of potential differences in chronic vs. acute silencing (44) and because previous work described how adaptation after changes in gravity progresses on the order of days rather than seconds (45, 46). We found that chronically inactivating Purkinje neuron GABA output has a significant effect on both spontaneous spiking variability (Fig. 4) as well as response magnitude to vestibular motion (Fig. 5). Purkinje neuron feedback is central to the control of various cell types within the cerebellar cortex. For the vestibular system, this involves secondary projections from Purkinje neurons to vestibular nuclear neurons, then back into the granule cell layer as mossy fibers (27). Additionally, Purkinje neurons project primary feedback collaterals that are especially pronounced in lobules IX-X (19, 20). Both of these projection types could contribute to the altered gain, either through disinhibition of excitatory vestibular nuclear neurons or of other Purkinje neurons. Moreover, vestibulo-cerebellar Purkinje neurons project to motion-responsive brainstem nuclei, which then project to the inferior olive (47). The inferior olive in turn has profound effects on Purkinje neuron firing. We did not observe differences in adult $L7^{Cre};Vgat^{flox/flox}$ spontaneous complex spike firing, but it remains possible that the cortico-nucleo-olivary loop is affected by the loss of Purkinje neuron signaling throughout development, potentially leading to "learning" an incorrect model of self-motion. We also found potential differences in phase of response to vestibular motion after blocking Purkinje neuron output. It would be informative in future work to use nonsinusoidal stimuli to determine whether these phase

clustering differences persist after genetic circuit manipulation. Overall, the striking increase in response gain to self-motion following Purkinje neuron output blockade suggests that they may play a key role in regulating appropriate vestibular activity levels, similar to gain control seen in other sensory systems (48–50).

In summary, the present results demonstrate that the process by which vermal Purkinje neurons carry a model of gravitational and linear acceleration is evolutionarily conserved and widespread across multiple lobules of the rodent vermis. Further, we show that genetic silencing of Purkinje neuron GABAergic output leaves this computational ability intact, but leads to increased response modulation amplitude. These findings suggest that the output of the cerebellar cortex, carried through both Purkinje neuron projections and collaterals, is critical in maintaining circuit firing at appropriate levels. These results highlight the highly conserved nature of vestibular processing, and suggest at least one function of Purkinje neuron signaling back to the cerebellar cortex: Purkinje neuron feedback may regulate gain control within the cerebellar circuit.

Materials and Methods

Detailed descriptions of methods are presented in *SI Appendix*.

Recordings. All experiments were approved by the Institutional Animal Care and Use Committee at Baylor College of Medicine. C57Bl/6J and $L7^{Cre}$; $Vgat^{flox/flox}$ mice colonies were maintained in our facility. Acute in vivo recordings were performed on restrained adult mice with surgically implanted head plates and craniotomy chambers. All data were collected by the same experimenter. Motion stimuli followed published protocols (14–17).

Analysis. Spiking activity across all stimuli trials for a cell was analyzed via linear regression for gain and phase response to tilt and translation motion, following published procedures (17, 24). Briefly, neuronal activity was converted into a spike density function, then each cycle was fit with a cosine function, with a complex number representing gain and phase. This complex number was regressed on the independent stimuli components. Spontaneous statistics were calculated from rest periods between stimuli. Reconstruction of recording sites was done post hoc via stereotaxic recording coordinates in reference to electrolytic lesions.

ACKNOWLEDGMENTS. We thank M. Shinder, N. Rotem, T. Lin, other D.E.A. and R.V.S. lab members, and Baylor College of Medicine animal care associates for their help. T.L.S. was supported by National Institute of Neurological Diseases and Stroke (NINDS) Grant F31NS095491; R.V.S. by National Institute of Child Health and Human Development Grant U54HD083092 and NINDS Grants R01NS089664 and R01NS100874; and D.E.A. by NINDS Grant NS098146. D.E.A. was also supported by Simons Foundation Grant 542949.

1. Fetsch CR, Deangelis GC, Angelaki DE (2010) Visual-vestibular cue integration for heading perception: Applications of optimal cue integration theory. *Eur J Neurosci* 31: 1721–1729.
2. Oman CM (1991) Sensory conflict in motion sickness. *Pictorial Communication in Real and Virtual Environments*, ed Ellis S (Taylor and Francis, London), pp 362–367.
3. Merfeld DM (1995) Modeling the vestibulo-ocular reflex of the squirrel monkey during eccentric rotation and roll tilt. *Exp Brain Res* 106:123–134.
4. Merfeld DM, Zupan L, Peterka RJ (1999) Humans use internal models to estimate gravity and linear acceleration. *Nature* 398:615–618.
5. Angelaki DE, McHenry MQ, Dickman JD, Newlands SD, Hess BJ (1999) Computation of inertial motion: Neural strategies to resolve ambiguous otolith information. *J Neurosci* 19:316–327.
6. Laurens J, Droulez J (2007) Bayesian processing of vestibular information. *Biol Cybern* 96:389–404.
7. Laurens J, Angelaki DE (2011) The functional significance of velocity storage and its dependence on gravity. *Exp Brain Res* 210:407–422.
8. Carpenter MB, Stein BM, Peter P (1972) Primary vestibulocerebellar fibers in the monkey: Distribution of fibers arising from distinctive cell groups of the vestibular ganglia. *Am J Anat* 135:221–249.
9. Korte GE, Mugnaini E (1979) The cerebellar projection of the vestibular nerve in the cat. *J Comp Neurol* 184:265–277.
10. Gerrits NM, Epema AH, van Linge A, Dalm E (1989) The primary vestibulocerebellar projection in the rabbit: Absence of primary afferents in the flocculus. *Neurosci Lett* 105:27–33.
11. Barmack NH, Baughman RW, Errico P, Shojaku H (1993) Vestibular primary afferent projection to the cerebellum of the rabbit. *J Comp Neurol* 327:521–534.
12. Maklad A, Fritzsch B (2003) Development of vestibular afferent projections into the hindbrain and their central targets. *Brain Res Bull* 60:497–510.
13. Maklad A, Kamel S, Wong E, Fritzsch B (2010) Development and organization of polarity-specific segregation of primary vestibular afferent fibers in mice. *Cell Tissue Res* 340:303–321.
14. Angelaki DE, Shaikh AG, Green AM, Dickman JD (2004) Neurons compute internal models of the physical laws of motion. *Nature* 430:560–564.
15. Yakusheva TA, et al. (2007) Purkinje cells in posterior cerebellar vermis encode motion in an inertial reference frame. *Neuron* 54:973–985.
16. Laurens J, Meng H, Angelaki DE (2013) Computation of linear acceleration through an internal model in the macaque cerebellum. *Nat Neurosci* 16:1701–1708.
17. Laurens J, Meng H, Angelaki DE (2013) Neural representation of orientation relative to gravity in the macaque cerebellum. *Neuron* 80:1508–1518.
18. Chaumont J, et al. (2013) Clusters of cerebellar Purkinje cells control their afferent climbing fiber discharge. *Proc Natl Acad Sci USA* 110:16223–16228.
19. Guo C, et al. (2016) Purkinje cells directly inhibit granule cells in specialized regions of the cerebellar cortex. *Neuron* 91:1330–1341.
20. Witter L, Rudolph S, Pressler RT, Lahlaf SI, Regehr WG (2016) Purkinje cell collaterals enable output signals from the cerebellar cortex to feed back to Purkinje cells and interneurons. *Neuron* 91:312–319.
21. White JJ, et al. (2014) Cerebellar zonal patterning relies on Purkinje cell neurotransmission. *J Neurosci* 34:8231–8245.
22. Carriot J, Jamali M, Chacron MJ, Cullen KE (2017) The statistics of the vestibular input experienced during natural self-motion differ between rodents and primates. *J Physiol* 595:2751–2766.
23. Green AM, Shaikh AG, Angelaki DE (2005) Sensory vestibular contributions to constructing internal models of self-motion. *J Neural Eng* 2:S164–S179.
24. Laurens J, Angelaki DE (2016) How the vestibulocerebellum builds an internal model of self-motion. *The Neuronal Codes of the Cerebellum*, ed Heck D (Academic, Cambridge, UK), pp 97–115.
25. Ozol K, Hayden JM, Oberdick J, Hawkes R (1999) Transverse zones in the vermis of the mouse cerebellum. *J Comp Neurol* 412:95–111.
26. Sillitoe RV, Hawkes R (2002) Whole-mount immunohistochemistry: A high-throughput screen for patterning defects in the mouse cerebellum. *J Histochem Cytochem* 50: 235–244.
27. Barmack NH (2003) Central vestibular system: Vestibular nuclei and posterior cerebellum. *Brain Res Bull* 60:511–541.
28. McIntire SL, Reimer RJ, Schuske K, Edwards RH, Jorgensen EM (1997) Identification and characterization of the vesicular GABA transporter. *Nature* 389:870–876.
29. Chaudhry FA, et al. (1998) The vesicular GABA transporter, VGAT, localizes to synaptic vesicles in sets of glycinergic as well as GABAergic neurons. *J Neurosci* 18:9733–9750.
30. Fujii M, et al. (2007) Respiratory activity in brainstem of fetal mice lacking glutamate decarboxylase 65/67 and vesicular GABA transporter. *Neuroscience* 146:1044–1052.
31. Saito K, et al. (2010) The physiological roles of vesicular GABA transporter during embryonic development: A study using knockout mice. *Mol Brain* 3:40.
32. Carleton SC, Carpenter MB (1984) Distribution of primary vestibular fibers in the brainstem and cerebellum of the monkey. *Brain Res* 294:281–298.
33. Naito Y, Newman A, Lee WS, Beykirch K, Honrubia V (1995) Projections of the individual vestibular end-organs in the brain stem of the squirrel monkey. *Hear Res* 87:141–155.
34. Yakhnitsa V, Barmack NH (2006) Antiphasic Purkinje cell responses in mouse uvula-nodulus are sensitive to static roll-tilt and topographically organized. *Neuroscience* 143:615–626.
35. Barmack NH, Yakhnitsa V (2008) Distribution of granule cells projecting to focal Purkinje cells in mouse uvula-nodulus. *Neuroscience* 156:216–221.
36. Barmack NH, Yakhnitsa V (2011) Topsy turvy: Functions of climbing and mossy fibers in the vestibulo-cerebellum. *Neuroscientist* 17:221–236.
37. Dugué GP, Tihy M, Gourévitch B, Léna C (2017) Cerebellar re-encoding of self-generated head movements. *eLife* 6:e26179.
38. Dow RS (1938) Effect of lesions in the vestibular part of the cerebellum in primates. *Arch Neurol Psy* 40:500–520.
39. Tarnutzer AA, Shaikh AG, Palla A, Straumann D, Marti S (2011) Vestibulo-cerebellar disease impairs the central representation of self-orientation. *Front Neurol* 2:11.
40. Eisenman LM (2011) Ethanol and vestibular stimulation reveal simple and complex aspects of cerebellar heterogeneity. *Cerebellum* 10:475–483.
41. Wylie DR, Pakan JM, Huynh H, Graham DJ, Iwaniuk AN (2012) Distribution of zebrin-immunoreactive Purkinje cell terminals in the cerebellar and vestibular nuclei of birds. *J Comp Neurol* 520:1532–1546.
42. Sillitoe RV, Joyner AL (2007) Morphology, molecular codes, and circuitry produce the three-dimensional complexity of the cerebellum. *Annu Rev Cell Dev Biol* 23:549–577.
43. Cerminara NL, Lang EJ, Sillitoe RV, Apps R (2015) Redefining the cerebellar cortex as an assembly of non-uniform Purkinje cell microcircuits. *Nat Rev Neurosci* 16:79–93.
44. Otchy TM, et al. (2015) Acute off-target effects of neural circuit manipulations. *Nature* 528:358–363.
45. Oman CM, Balkwill MD (1993) Horizontal angular VOR, nystagmus dumping, and sensation duration in spacelab SLS-1 crewmembers. *J Vestib Res* 3:315–330.
46. Young LR, Sinha P (1998) Spaceflight influences on ocular counterrolling and other neurovestibular reactions. *Otolaryng Head Neck Surg* 118(Suppl 3):S31–S34.
47. Barmack NH, Fredette BJ, Mugnaini E (1998) Parasolitary nucleus: A source of GABAergic vestibular information to the inferior olive of rat and rabbit. *J Comp Neurol* 392:352–372.
48. Hudspeth AJ (2008) Making an effort to listen: Mechanical amplification in the ear. *Neuron* 59:530–545.
49. Root CM, et al. (2008) A presynaptic gain control mechanism fine-tunes olfactory behavior. *Neuron* 59:311–321.
50. Olsen SR, Bortone DS, Adesnik H, Scanziani M (2012) Gain control by layer six in cortical circuits of vision. *Nature* 483:47–52.